

Magnetic and structural properties of $\text{II}^{\text{A-V}}$ nitrides

O. Volnianska and P. Bogusławski

Institute of Physics, Polish Academy of Sciences, 02-668 Warsaw, Poland

(Received 19 July 2006; revised manuscript received 1 March 2007; published 14 June 2007)

Electronic, magnetic, and structural properties of several $\text{II}^{\text{A-V}}$ compounds are analyzed using *ab initio* calculations. We consider four crystal structures: zinc-blende, NiAs, rocksalt, and Zn_3P_2 . Our results indicate that $\text{II}^{\text{A-V}}$ nitrides in the rocksalt phase are stable ferromagnetic half-metals characterized by the total spin polarization of free holes in the valence band. The previously considered zinc-blende phase of II-V crystals is ferromagnetic as well, but is less stable by about 0.3 eV/atom. The stability of the Zn_3P_2 phase is close to that of the rocksalt, but the spin polarization vanishes in this case. Analysis of the electronic structure shows that ferromagnetism of $\text{II}^{\text{A-V}}$ compounds originates in the spin polarization of the p shell of anions, as described by Hund's rule, which persists in solids after formation of bonds. Furthermore, the results for isolated atoms indicate why the spin polarization is the most stable in $\text{II}^{\text{A-V}}$ nitrides, which are discussed in detail.

DOI: 10.1103/PhysRevB.75.224418

PACS number(s): 75.50.Cc, 71.15.Mb

I. INTRODUCTION

In various classes of magnetic systems, magnetism is due to the presence of cations with partially occupied d or f shells. Recently, it was proposed that spin polarization may exist in solids that do not contain transition-metal or rare-earth atoms. Observation of ferromagnetism (FM) in CaB_6 (Refs. 1 and 2) was initially explained as an intrinsic property of the free-electron gas.³ However, the origin of FM in CaB_6 , as well as in HfO_2 ,⁴ is currently under debate that tentatively ascribes the effect to the presence of lattice defects,² or magnetic inclusions.⁵ For example, Moriwaka *et al.* propose that ferromagnetism of $(\text{Ca}, \text{La})\text{B}_6$ is induced by Ca vacancies.⁶ In fact, vacancies and other defects in insulators typically introduce deep levels in the band gap, and electrons that occupy these levels form states with total spin 0 or 1/2. However, in some cases, electrons assume high-spin configurations, i.e., their spins are arranged parallel in accord with Hund's rule. This is the case of the silicon vacancy in SiC, for which the spin-spin exchange interaction is large: the experimentally observed state of the negatively charged vacancy is a high-spin configuration with spin 3/2.⁷ This configuration is obtained by first-principles calculations as well.⁸ The high-spin ground state is also observed for the neutral Ga vacancy in GaP.⁹ The same effect may take place for the Ca vacancy in CaO, which assumes the high-spin state according to calculations of Elfimov *et al.*¹⁰ These examples demonstrate that in some cases, the exchange coupling is strong enough to induce high-spin (i.e., spin-polarized) local configurations, which are related to s and p rather than with d atomic orbitals. Moreover, for a sufficiently high concentration of such defects and a nonvanishing coupling between them, a macroscopic magnetic order is expected. Recently, Kenmochi *et al.*¹¹ have proposed that such an effect takes place in II-VI oxides. According to their calculations, MgO, CaO, and SrO containing a few percent of C, which is a double acceptor when substituting O, is ferromagnetic due to the spin polarization of carriers in the C-induced impurity band.

Intensive studies are also devoted to magnetism in organic materials without transition-metal atoms.^{12–22} Several works reported the observation of ferromagnetism in, e.g., C_{60} -

based polymers,^{12–14} graphite-based materials,^{15–17} and provided theoretical models for this effects.^{18–21} Ferromagnetism in these systems is weak, since typical Curie temperatures T_C do not exceed 15 K. Possible origins of FM are nucleation of local moments at lattice defects, “ordered disorder” (e.g., sp^2 - sp^3 mixtures), or the presence of hydrogen.²²

In search of ferromagnetic materials without transition-metal ions, Kukasabe *et al.*²³ have analyzed CaP, CaAs, and CaSb in the zinc-blende (zb) structure and found that they are half-metals with a total spin polarization of holes in the valence band. Properties of several II-V compounds have been further explored by Sieberer *et al.*²⁴ and by the present authors²⁵ who showed that a number of II-V crystals are half-metals. (Half-metals are metals with a total spin polarization of free carriers, such as several Heusler alloys.) The obtained results confirmed the presence and stability of the ferromagnetic phase in this family of materials. (For the sake of brevity, we refer to the spin-polarized and spin-unpolarized phases as ferro- and paramagnetic, and denote them by FM and PM, respectively.) Kukasabe *et al.*²³ have attributed FM to a large contribution of $d(\text{Ca})$ orbitals to the bonds, while Seiberer *et al.*²⁴ explain the effect by the so-called flatband magnetism of holes.

However, the zb structure analyzed in detail in Refs. 23–25 is not the stable crystalline structure of these compounds. The question, therefore, arises what are the stable phases, and whether the spin polarization persists in these structures. In fact, in contrast to III-V or II-VI compounds that typically crystallize in the zb structure, II-V compounds crystallize in variety of structures, the most common being Zn_3P_2 or a more complex Zn_3As_2 phases.²⁶ Magnetic $\text{II}^{\text{TM-V}}$ compounds (where II^{TM} is a transition-metal ion) usually crystallize in the NiAs structure. SrN has been observed both in the rocksalt²⁷ (rs) and in the monoclinic²⁸ structure. Consequently, we consider here four structures: zb, rs, NiAs, and Zn_3P_2 . A detailed analysis is performed for the most interesting rs phase, since according to the obtained results the rs- $\text{II}^{\text{A-V}}$ nitrides are FM. The rs structure is metastable, since the corresponding heats of formation are somewhat higher than those of the Zn_3P_2 phase. The energies of both the zb and the NiAs phases are about 0.3 eV/atom higher. Next, we

TABLE I. Energies of spin polarization $\Delta E^{\text{FM-PM}}$ (in meV per two atoms), i.e., the energy difference between the spin-polarized and spin-unpolarized phases for rs, NiAs, and zb structures, and differences in energies $\Delta E^{\text{FM-AFM}}$ (in meV per two atoms) of FM and AFM phases. The last column gives energies of spin polarization of isolated group-V atoms (in eV).

	$\Delta E^{\text{FM-PM}}$ (crystal)			$\Delta E^{\text{FM-AFM}}$ (crystal)		$\Delta E^{\text{FM-PM}}$ (anion)
	rs	NiAs	zb	rs	zb	
BaN	-90	-105	-125	-5	-45	
SrN	-135	-205	-185	-35	-50	
CaN	-140	-125	-195	-65	-50	-2.45
CaP	-3	0	-55	0		-1.37
CaAs	0	0	-40			-1.24
CaSb	0	0	-5			-1.02

identify the mechanism of stabilization of spin polarization in both the rs- and zb-II^A-V nitrides, which is the spin polarization of isolated anions. Since the spin polarization of anions is the strongest for light C, N, and O atoms, this mechanism may also explain the high-spin states of vacancies in SiC and CaO, and ferromagnetism of CaO:C. The strong exchange interaction that induces the high-spin polarization is due to the compactness of both *s* and *p* orbitals of atoms from the second row of the Periodic Table.

Finally, apart from its basic character, the problem of magnetism without transition-metal ions is of interest in the context of spintronic application. In recent years, there have been a number of discoveries in this area allowing to propose other types of devices, in which the spin degrees of freedom rather than the electron charge are used to generate, convey, and store information.²⁹ Currently investigated diluted magnetic III-V and II-VI semiconductors are characterized by Curie temperatures T_C that achieve about 170 K.^{29,30} An important exception is ZnSe:Cr with T_C exceeding the room temperature.³¹ Ferromagnetic epitaxial layers of half-metallic CaN, SrN, and BaN grown on III-V or II-VI semiconductors may potentially be attractive as spin injectors. This is because one may expect injection efficiency similar to that of half-metallic Heusler alloys used in the recently studied hybrid ferromagnet/semiconductor structures.^{32,33} In particular, this may be the case of II^A-N/III-N nitride heterojunctions, where valence states in both compounds are mainly formed from *p*(N) orbitals.

The paper is organized as follows. In Sec. II, we briefly present the computational methodology. The main problem of this paper, which are the magnetic properties of II^A-V compounds, is analyzed in detail in Sec. III for four crystalline structures. In Sec. IV, we discuss relative stability of various crystalline phases, their cohesive energies, heats of formation, and lattice parameters. Section V summarizes our results and concludes the paper.

II. METHODOLOGY

The calculations have been performed within the framework of density-functional theory. The exchange and correlation effects have been treated using both the local spin

density (LSDA) and the generalized gradient (GGA) approximations.³⁴ Similar results were obtained using both approximations. For II^A-N crystals, we present the results obtained within the GGA, which typically is more accurate for magnetic systems. We have employed ESPRESSO code,³⁵ ultrasoft atomic pseudopotentials,³⁶ and the plane-wave basis with the kinetic-energy cutoff of 35 Ry, which provided a good description of III-N nitrides, such as GaN and (Ga,Mn)N,³⁷ that are similar to II^A-V compounds studied here. Orbitals that were chosen as valence orbitals are *3s*, *3p*, *4s*, *3d* for Ca, *4s*, *4p*, *4d*, *5s*, *5p* for Sr, *5s*, *5p*, *5d*, *6s*, *6p* for Ba, *2s*, *2p* for N, *3s*, *3p* for P, *4s*, *4p* for As, and *5s*, *5p* for Sb. Brillouin-zone integrations were performed using a regular mesh of $(12 \times 12 \times 12)$ *k* points for zb and rs structures, and equivalent meshes for other structures.

III. MAGNETIC PROPERTIES AND ELECTRONIC STRUCTURE OF II^A-V COMPOUNDS

The calculated magnetic properties of the considered compounds at equilibrium are summarized in Table I, which gives the difference in energies of the spin-polarized and spin-unpolarized phases, $\Delta E^{\text{FM-PM}}$, for all investigated crystals, as well as the difference in energies of FM and antiferromagnetic (AFM) phases, $\Delta E^{\text{FM-AFM}}$. First, we see that the spin polarization of the considered compounds in the zb structure is nonvanishing. This result holds for SrAs and BaAs as well. On the other hand, zb-MgP, zb-MgAs,^{24,25} and all zb-Be-V (Ref. 24) crystals are paramagnetic. Next, as it follows from the table, in both the rs and the NiAs structure only the II-nitrides are FM. Finally, independent of the crystal structure, the calculated magnetic moment per two atoms μ is always equal to $1\mu_B$ in the FM phase. A borderline case is rs-CaP, for which the very small $\Delta E^{\text{FM-PM}} = -3$ meV is practically vanishing within our numerical accuracy, consistently with its small magnetic moment, $0.2\mu_B$. In contrast, Ca₃N₂, Sr₃N₂, and Ba₃N₂ in the Zn₃P₂ structure are paramagnetic.

As mentioned in Sec. II, GGA and LSDA give similar results. For example, in the case of zb-CaP, the LSDA and GGA lattice constants differ by 5%, and the absolute value of the energy of spin polarization $|\Delta E^{\text{FM-PM}}|$ obtained in LSDA

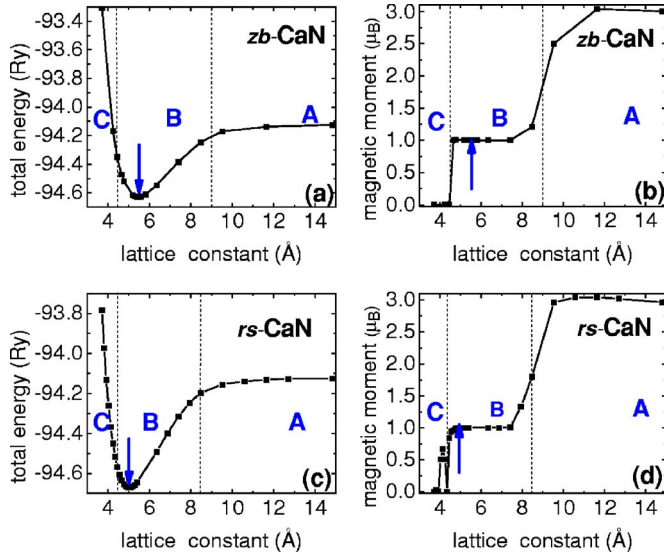


FIG. 1. (Color online) Total energy and total magnetic moment per unit cell as function of the lattice constant of zb-CaN [(a) and (b)] and rs-CaN [(c) and (d)]. Arrows indicate the equilibrium lattice constants a_{eq} .

is lower by 40 meV than that in GGA, consistently with $|\Delta E^{\text{FM-PM}}|$ of isolated P being lower by 0.26 eV in LSDA (see Sec. III B for discussion). For the rs-CaP, $\Delta E^{\text{FM-PM}}$ calculated using LSDA and GGA are the same within our accuracy. In the case of rs-CaN, the LSDA and GGA lattice constants differ by about 10%, while $\Delta E^{\text{FM-PM}}$ are -140 and -137 meV, respectively.

We have also investigated the relative stability of FM and AFM phases. The calculations were performed only for the most interesting cases of rs and zb phases of $\text{II}^{\text{A}}\text{-N}$ nitrides. (This is because the NiAs structure is less stable than rs, see Sec. IV, and spin polarization of other rs- $\text{II}^{\text{A}}\text{-V}$ crystals vanishes.) To this end, we considered the type-I AFM ordering, in which spins of anions in every (001) plane are parallel, but the sign of the polarization of consecutive planes alternates.³⁸ The calculated differences between energies of FM and AFM phases, $\Delta E^{\text{FM-AFM}}$, are given in Table I. The results show that in all crystals, the FM phase is the ground-state magnetic order. Furthermore, the absolute values of $\Delta E^{\text{FM-PM}}$ are higher than those of $\Delta E^{\text{FM-AFM}}$. This shows that with the increasing temperature, spin polarization should vanish as a result of the disordering of the magnetic moments, and not of their disappearance.

To understand the obtained magnetic properties, we will follow the formation of a $\text{II}^{\text{A}}\text{-V}$ crystal beginning from the case of isolated atoms to that of a compressed solid. The calculated total energies and the magnetic moments of zb- and rs-CaN are shown in Fig. 1. These results are typical for all the considered $\text{II}^{\text{A}}\text{-V}$ crystals. One may see that there are three ranges of lattice constants characterized by qualitatively different properties, for which the magnetic moment per unit cell is $3\mu_B$, $1\mu_B$, and $0\mu_B$, and denoted as A, B, and C, respectively. We will now discuss these cases beginning with that of large lattice constants.

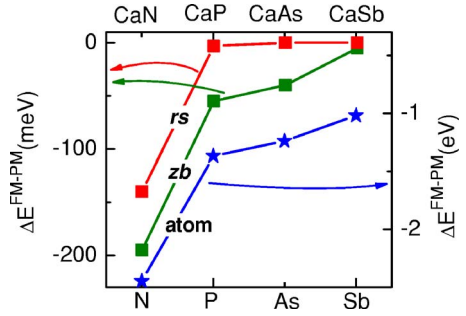


FIG. 2. (Color online) Difference in energies of FM and PM phases $\Delta E^{\text{FM-PM}}$ for CaX compounds in the rs and zb structures and for isolated anions. The lines are to guide the eye.

A. Case A: Isolated atoms

When the lattice constant a is very large, about 15 \AA (case A in Fig. 1), the atoms are practically isolated. Consequently, the properties of the system, such as the total energy or energy levels, correspond to a superposition of atomic properties. In particular, the magnetic moment is $3\mu_B$ per unit cell, owing to the fact that the magnetic moment of group-II Ca vanishes, while that of N and other group-V anions is $3\mu_B$, since three electrons that occupy p orbitals have parallel spins according to Hund's rule.

B. Case B: $\text{II}^{\text{A}}\text{-V}$ compounds at equilibrium

With the decreasing lattice constant, the atoms begin to interact and form bonds. This leads to a decrease of the total energy and to a drop of the magnetic moment from $3\mu_B$ to $1\mu_B$. Figure 1 shows that the onset of formation of bonds (displayed by the decrease of the total energy) is correlated with the drop of magnetization, which occurs at $\sim 9 \text{ \AA}$ for zb-CaN and $\sim 8.5 \text{ \AA}$ for rs-CaN. The magnetic moment is then constant for $4.5 \text{ \AA} < a < 9 \text{ \AA}$ for the zb or $3.7 \text{ \AA} < a < 8.5 \text{ \AA}$ for the rs phase, respectively. The drop of the magnetic moment is due to the changes in the electronic structure and charge-transfer effects induced by formation of bonds. A detailed analysis of the electronic structure is presented below.

1. Atomic origin of spin polarization

We begin with the most important question about the origin of the ferromagnetism found for several $\text{II}^{\text{A}}\text{-V}$ crystals. The answer is given by analysis of their electronic structure. From Table I, it follows that in the series of Ca compounds (CaN, CaP, CaAs, CaSb) in the zb phase, the energy of spin polarization is the largest for CaN, -195 meV, it decreases with the increasing atomic number of the anion, and almost vanishes for CaSb. This indicates that anions play an important role in determining the spin polarization of these compounds. This suggestion is supported by Fig. 2, which shows $\Delta E^{\text{FM-PM}}$ of crystals and of isolated anions. One may see that the energies of spin polarization of anions decrease from -2.45 eV for N to -1.02 eV for Sb,³⁹ which correlates well with the trend found for zb-II-V compounds. Moreover, $\Delta E^{\text{FM-PM}}$ is about twice higher for N than for the remaining anions, which may be the cause of the stability of the FM

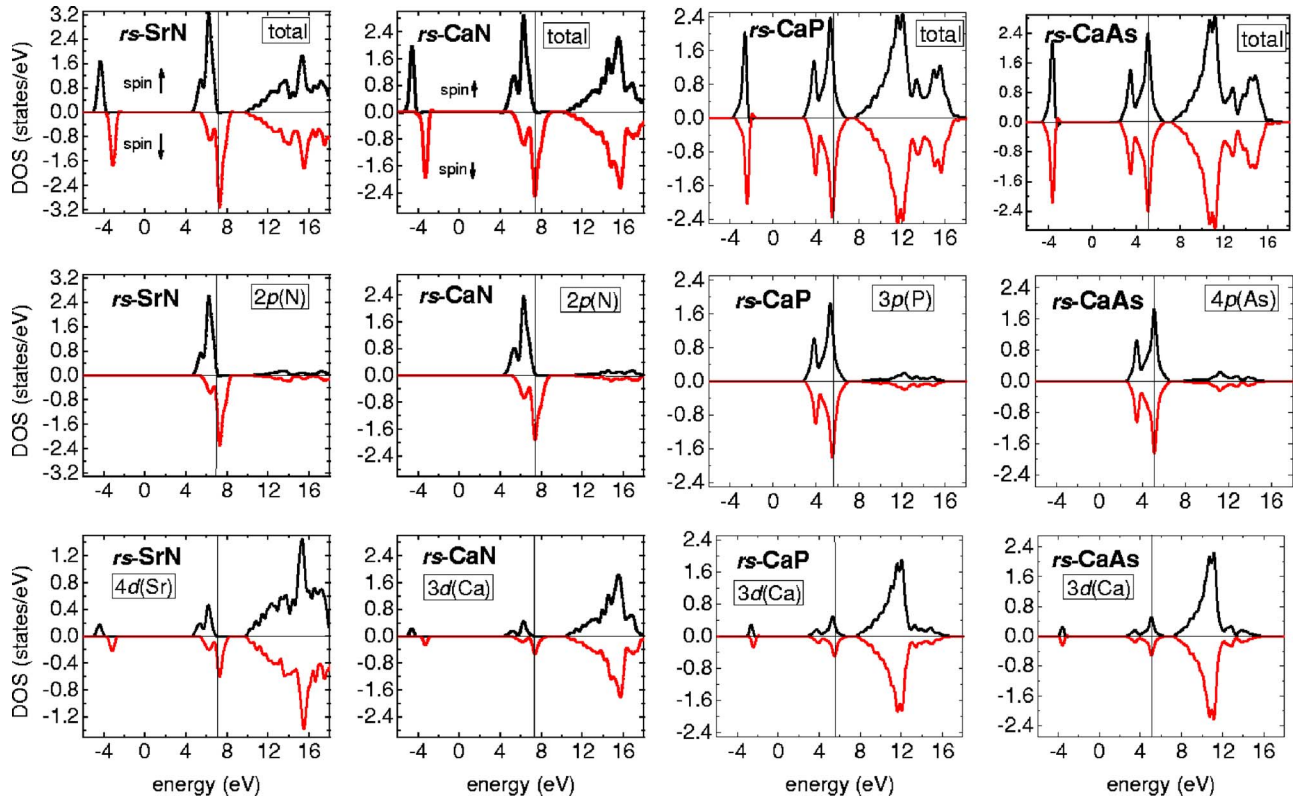


FIG. 3. (Color online) Density of states per unit cell of SrN, CaN, CaP, and CaAs in the rs structure. Both the total DOS and the contributions of p and d orbitals are given. Vertical lines show the Fermi energy. Positive and negative values of DOS hold for spin-up and spin-down states, respectively.

order in the NiAs and rs structures of the nitrides.

This hypothesis is confirmed by the analysis of the density of states (DOS) and of projection of the wave function on atomic orbitals shown in Fig. 3 for SrN, CaN, CaP, and CaAs in the rs structure. In all cases, the top of the valence band is mainly formed from the p orbitals of anions, which contribute about 75%. The contribution of d orbitals of cations to the valence bands is at least five times smaller. These orbitals (which are the lowest excited states of cations) contribute mainly to the higher conduction states. In particular, they give rise to a $d(\text{Ca})$ -derived bands at about 4–8 eV above the bottom of the conduction band. The spin polarization of SrN and CaN is visible; one may also see a very weak polarization in CaP, while that of CaAs vanishes. Very similar results are obtained for the zb phase in spite of differences in the detailed dispersions of energy bands.

Figure 4 confirms the conclusion that the spin polarization of crystals results from the spin polarization of the p (anion) states. The contour plot of the spin density displayed in Fig. 4 for both zb- and rs-CaN shows that the spin polarization is strongly localized in the vicinity of N atoms. In accord with Fig. 3, the contribution of Ca states is visible, but small. Qualitatively identical results are obtained for BaN and SrN. Finally, we note that a large contribution of the $d(\text{Ca})$ states to the valence bands could, in principle, explain the magnetism of II-V compounds, which would then have an origin similar to that in systems containing transition-metal atoms. This explanation was suggested by Kukasabe *et al.*²³ However, the obtained results show that this is not the case.

2. Energy bands and magnetic moments at equilibrium

The calculated band structures of CaN, CaP, CaAs, SrN, and BaN in the rs phase at equilibrium are shown in Fig. 5. (The energy bands of CaN in both zb and NiAs structures were shown in Ref. 25.) Energy bands of CaSb are similar to these of CaAs. With the decreasing lattice constant from case A of isolated atoms to case B, the electrons begin to form chemical bonds. In particular, the bonding combination of $p(\text{N})$ with Ca orbitals decreases in energy and forms the Γ_{15} top of the valence bands, while the antibonding combination of $s(\text{Ca})$ with $s(\text{N})$ and $p(\text{N})$ orbitals rises in energy and forms the bottom of the conduction band, see Fig. 5. Consequently, two electrons are transferred from $s(\text{Ca})$ -derived to spin-down $p(\text{N})$ -derived states, reducing the magnetic moment from 3 to 1.

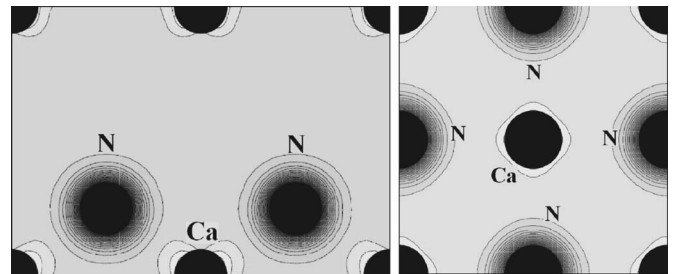


FIG. 4. Contour plots of the calculated spin density for zb-CaN in the (110) plane (left panel), and rs-CaN in the (001) plane (right panel).

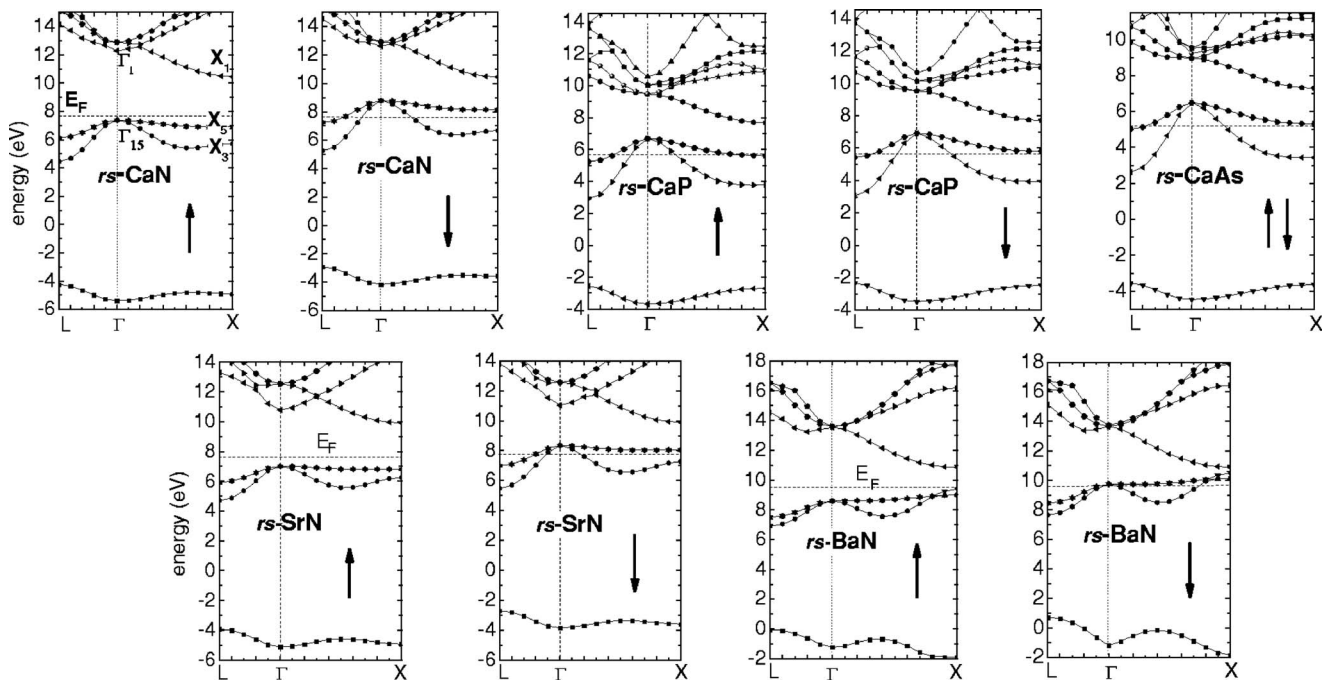


FIG. 5. Band structures of rs CaN, CaP, CaAs, SrN, and BaN at equilibrium. Arrows denote the spin-up and spin-down channels, and horizontal dashed lines indicate the Fermi energy.

Figure 5 shows that energy bands of rs-II-V compounds compared with those of typical III-V or II-VI crystals in the zb phase exhibit characteristic differences.

(i) II-V crystals have seven valence electrons per unit cell, and thus they are not insulators but metals with one free hole per cell.

(ii) In all FM II-V nitrides, the free hole gas is fully spin polarized, and therefore these crystals at equilibrium are half-metals. As it was mentioned above, in CaP, spin polarization is very small. Finally, in CaAs, the holes are not spin polarized, and this compound is a paramagnetic metal.

(iii) The valence bands of CaN, CaP, and CaAs are similar in shape to these of, e.g., a typical III-V compound GaAs. On the other hand, the structure of the conduction bands is different. In particular, there are additional bands that originate in the $3d(\text{Ca})$ orbitals, which are also seen in Fig. 3. Moreover, the bottom of the conduction band occurs at the X point of the Brillouin zone.

(iv) In the series CaN, SrN, and BaN, there is an interesting trend consisting in the change of relative energies at the Γ and X points. Namely, in CaN, the curvature of the highest valence bands along the Γ -X direction is small, but the maximum of this band occurs at Γ . In the case of both SrN and BaN, the band maximum is shifted from Γ to X. Consequently, in these two compounds, the gap has a direct character, but the gap minimum occurs at the X point. Moreover, the minimum of the lower valence band situated about 10–12 eV below the top of the valence band is shifted from Γ to X. The small dispersions and atypical shapes of the valence bands result mainly from the large values of the lattice constant due to the large atomic radii of the heavy Ca, Sr, and Ba cations. Moreover, since the top of valence band is mainly formed from $p(\text{N})$ orbitals that have a small atomic

radius, the overlap between cations, i.e., second neighbors, may play an important role in determining the actual dispersion of these bands. Interestingly, however, the fact that in the nitrides the minimum of the direct band gap that occurs at the X point is reproduced by simple model calculations based on the approach of Harrison.⁴⁰

According to the obtained results, rs-II-N nitrides are half-metals. Nevertheless, the flatness of the upper valence band may suggest that these systems are magnetic Mott-Hubbard insulators, similar to several transition-metal oxides in which strong electron correlations play a critical role. This possibility may be verified by calculations beyond LSDA that use methods appropriate for highly correlated systems. However, even if this would be the case, the main physical effect on which we focus here, i.e., the magnetism based on partially filled p (and not d or f) atomic shell, would remain valid.

Finally, the band structure of $\text{II}^{\text{A}}-\text{V}$ compounds in Zn_3P_2 phase is complex and “obscure” due to the fact that the unit cell contains 40 atoms with 128 valence electrons, which occupy 64 bands spanning an energy range of about 10 eV. For this reason, we do not show it. The most important result that should be pointed out is that Ca_3N_2 , Sr_3N_2 , and Ba_3N_2 are all insulators with the calculated band gaps of about 0.5 eV. The insulating character of these compounds follows, in particular, from the fact that there is an even number of electrons per unit cell. Consequently, there are no free holes and the spin polarization is zero.

C. Case C: Electronic structure at high pressures

We now turn to the FM-to-PM transition, i.e., to the destabilization of the spin polarization that occurs at suffi-

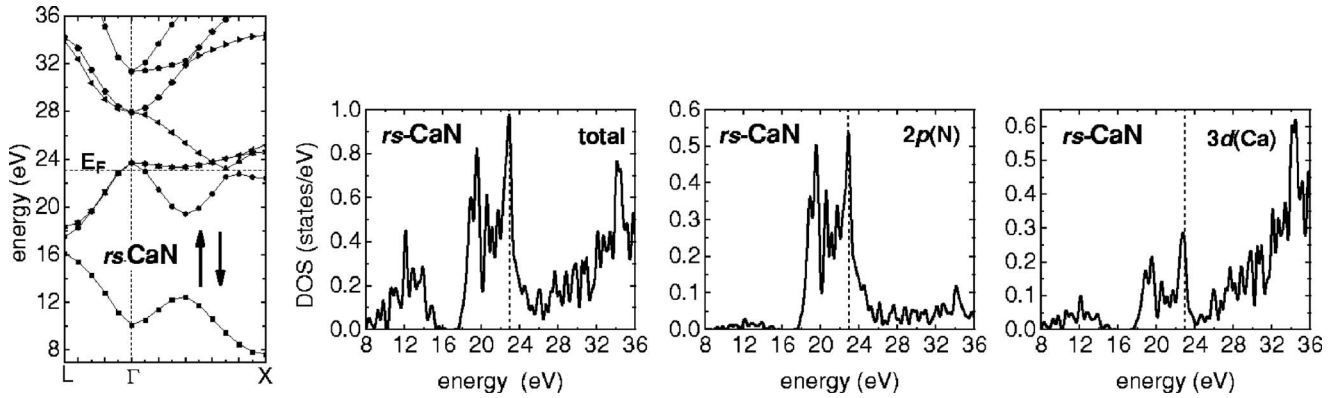


FIG. 6. Band structure of rs-CaN, and the total and partial densities of states at the critical lattice constant $a_{\text{crit}}=3.7 \text{ \AA}$. Dashed lines indicate the Fermi energy.

ciently small lattice constants for all the considered compounds. This transition is seen in Fig. 1 for CaN. In all cases, the disappearance of the magnetization is not accompanied with major and abrupt changes of the band structure, and the decreasing lattice constant induces a progressive decrease of the spin splitting, as well as an increase of the width of the valence bands. The pressure-induced disappearance of the spin polarization may qualitatively be understood based on the Stoner criterion.⁴¹ This criterion indicates that the stability of spin polarization is favored by large magnetic susceptibility, which is proportional the density of states at the Fermi level, and is destabilized by kinetic energy E_{kin} at high electron densities. These factors are briefly discussed below.

The FM-to-PM transition induced by external pressure has been analyzed for free-electron gas within quantum Monte Carlo calculations.^{3,42,43} In this model case, the difference in the kinetic energies of FM and PM phases is $0.17\hbar^2k_F^2/m_e$, which increases with the increasing pressure. In crystals, the destabilizing role played by E_{kin} is further enhanced by a second factor, namely, the decrease of the effective mass m^* of free carriers with the decreasing lattice constant. This effect originates in the increase of the bandwidths due to stronger interatomic interactions. These arguments hold also in $\text{II}^{\text{A}}\text{-V}$ crystals with the zinc-blende structure, where the valence bands have sinusoidal-like shapes to a good approximation. In particular, they may explain the lack of FM in zb-Be-V (Ref. 24) and zb-Mg-V (Ref. 25) compounds, which have lattice constants smaller than the corresponding compounds of Ca, Sr, and Ba.

However, the energy bands in rs-II-V nitrides have a more complex topology. As an example, Fig. 6 shows both the band structure and the DOS for rs-CaN at the critical lattice constant a_{crit} for which the spin polarization vanishes. (The values of a_{crit} are given in Table II below.) In this case, there is an overlap of the conduction and valence states. In the spirit of the Stoner criterion, the relevant quantity is the DOS at the Fermi level. A comparison of the results from Figs. 3 and 6 illustrates well this point, since the DOS at the Fermi level decreases almost three times when the lattice constant decreases from $a_{\text{eq}}=5.0$ to $a_{\text{crit}}=3.7 \text{ \AA}$, driving the destabilization of the FM phase.

IV. STRUCTURAL STABILITY OF $\text{II}^{\text{A}}\text{-V}$ COMPOUNDS

In contrast to III-V or II-VI compounds that typically crystallize in the zb structure, II-V compounds crystallize in variety of structures. Several II-V compounds assume the Zn_3P_2 phase, which is a primitive tetragonal lattice with 40 atoms in the unit cell, or a more complex Zn_3As_2 , which is a body-center tetragonal structure with 160 atoms in the unit cell.²⁶ Materials with these structures are not magnetic. SrN has been observed in two phases, namely, rs (Ref. 27) and monoclinic.²⁸ Magnetic $\text{II}^{\text{TM}}\text{-V}$ compounds (where II^{TM} is a transition-metal ion) usually crystallize in the NiAs structure. This is the case of NiAs, CrAs, CrSb,⁴⁴ and also of FM $\alpha\text{-MnAs}$ that crystallizes in the NiAs structure with alternating hexagonal planes of Mn and As atoms.⁴⁵ However, it is important to notice that with the help of epitaxial techniques of growth, it is possible to synthesize these compounds in other structures that are metastable. For example, CrAs (Ref. 46) and CrSb (Ref. 47) layers have been fabricated in the metastable zb structure by molecular-beam epitaxy in spite of the fact that the calculated total energy of this phase is at least 0.4 eV/atom higher than that of the ground-state NiAs phase.⁴⁸ Turning to the case of $\text{II}^{\text{TM}}\text{-V}$ nitrides, we observe that the early transition-metal mononitrides TiN and VN crystallize in the rocksalt structure.⁴⁹ In particular, rs-ScN,⁵⁰ rs-CeN,⁵¹ and rs-CrN (Ref. 52) were grown by sputter deposition on MgO(001) substrates. Finally, the ground-state phase of MnN is the rocksalt structure with a weak tetragonal distortion^{53,54} and AFM ordering, reproduced by first-principles calculations.^{55,56} The AFM ordering has also been found both for the zb (Ref. 57) and for the wurtzite⁵⁸ metastable structures of MnN. Because of the variety of possible structures of $\text{II}^{\text{A}}\text{-V}$ compounds, it is important to establish their low-energy phases. To this end, we investigate here four structures, namely, zb, NiAs, Zn_3P_2 , and rs. The wurtzite structure is not considered since its energy typically differs from that of zb by a few meV/atom only.

The calculated total energy as a function of the atomic volume for zb, rs, and the NiAs phases of CaN is presented in Fig. 7. It is not possible to present E_{tot} of CaN in the Zn_3P_2 structure in this figure because of the different stoichiometries of this phase. Figure 7 shows that the most stable

TABLE II. Calculated equilibrium lattice parameters, critical lattice constant a_{crit} (in Å), cohesive energies, and heats of formation of II^A-V compounds. For hexagonal phases, we give the values of both a_{eq} (in Å) and of c/a in two consecutive lines.

Phase	BaN	SrN	CaN	CaP	CaAs	CaSb
Lattice parameters at equilibrium						
zb	5.92	5.82	5.40	6.88	7.14	7.41
NiAs	3.81	3.65	3.49	4.02	4.13	4.23
	1.73	1.93	1.83	2.13	2.13	2.23
Zn ₃ P ₂	8.99	8.73	8.20			
	1.41	1.41	1.41			
rs	5.55	5.40	5.0	6.24	6.35	6.66
Critical lattice constant						
zb	4.8	4.87	4.5	5.3	5.8	6.88
rs	5.18	4.34	3.7	5.9	6.35	7.4
Cohesive energy (eV per two atoms)						
zb	-6.85	-6.16	-6.74	-5.38	-5.12	-4.71
NiAs	-6.82	-6.17	-6.89	-5.92	-5.73	-5.41
Zn ₃ P ₂	-7.19	-6.67	-7.63			
rs	-7.12	-6.78	-7.48	-6.20	-5.95	-5.53
Heat of formation (eV/atom)						
Zn ₃ P ₂	-1.05	-0.81	-1.55			
rs	-0.37	-0.26	-0.78			

phase is rs, while the zb phase is higher in energy by 0.75 eV/atom. These results characterize other II^A-V compounds as well, see Table II, and are similar to these obtained for ScN (Ref. 59) and CaAs.²⁴

The calculated lattice parameters are given in Table I, along with cohesive energies per two atoms defined as

$$E_{\text{coh}}^{\text{II-V}} = 2(E_{\text{tot}}^{\text{II-V}} - n^{\text{II}}E_{\text{at}}^{\text{II}} - n^{\text{V}}E_{\text{at}}^{\text{V}})/(n^{\text{II}} + n^{\text{V}}). \quad (1)$$

Here, $E_{\text{tot}}^{\text{II-V}}$ is the total energy per unit cell of the considered compound, E_{at} is the energy of isolated atom, and n^{II} and n^{V} are number of atoms of groups II and V in the unit cell, respectively. Considering first the simple structures, we find that for all compounds (except BaN) the zb phase is the

less stable, NiAs is intermediate, and rs is the most stable one.

Since we expect the magnetism to be the most stable for the II-V nitrides (see Sec. III), we have also considered the computationally more demanding Zn₃P₂ phase for these compounds. For both BaN and CaN, the Zn₃P₂ phase is more stable than the rs, with the difference in cohesive energies between the two phases of 0.032 and 0.075 eV/atom, respectively. In contrast, SrN in the rs phase is more stable by 0.055 eV/atom. The calculated cohesive energies of II-V nitrides are large compared to, e.g., $E_{\text{coh}}^{\text{II-V}}$ of Ca, which is -3.68 eV per two atoms. This indicates that after being formed, the II-N crystals are expected to be stable due to the high energies of II-N bonds.

A second aspect of stability of a compound is displayed by its heat of formation ΔH_f^0 , which indicates stability with respect to decomposition into bulk constituents. The heat of formation at $T=0$ K is obtained by considering the reaction to form (or decompose) a crystalline bulk II-nitride from (or into) its components, and is defined as

$$\Delta H_f^0 = E_{\text{coh}}^{\text{II-V}} - (n^{\text{II}}E_{\text{coh}}^{\text{II}} + n^{\text{N}}E_{\text{bind}}^{\text{N}_2}/2)/(n^{\text{II}} + n^{\text{V}}), \quad (2)$$

where $E_{\text{coh}}^{\text{II-V}}$ and $E_{\text{coh}}^{\text{II}}$ are the cohesive energy per atom of the considered nitrides and of the group-II metal in its equilibrium structure, respectively, and $E_{\text{bind}}^{\text{N}_2}$ is the binding energy of the N₂ dimer. The obtained results for $E_{\text{coh}}^{\text{II}}$ are -1.80, -1.62, and -1.85 eV/atom for Ca, Sr, and Ba in their equilibrium structures (fcc, fcc, and bcc, respectively). The calculated $E_{\text{bind}}^{\text{N}_2}$ is -4.9 eV/atom, in reasonable agreement with

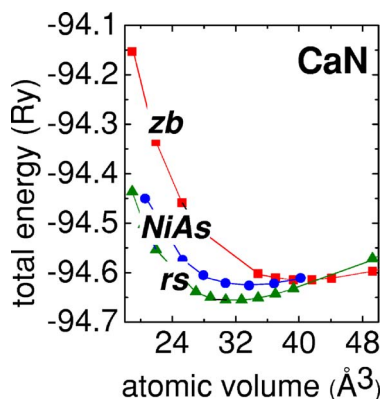


FIG. 7. (Color online) Total energy (in Ry per two atoms) as a function of the atomic volume for three structures of CaN.

experimental data. Note that according to this definition a negative ΔH_f^0 implies that the compound is stable with respect to decomposition into bulk constituents. The calculated values of E_{coh}^{II-V} and ΔH_f^0 are given in Table II. The results for BaN, SrN, and CaN show that the Zn_3P_2 structure is energetically more favorable than the rs phase, since its ΔH_f^0 is lower. From Table II, it follows that the differences between ΔH_f^0 of the Zn_3P_2 and the rs structure are 0.77, 0.55, and 0.68 eV for CaN, SrN, and BaN, respectively. However, we stress that not only the Zn_3P_2 but also the rs phase is thermodynamically stable, which follows from the negative ΔH_f^0 . Since the stoichiometries of these structures are different, the formation of one of them should critically depend on the conditions of growth. Consequently, the relative stability of the rs phase of II^A-V nitrides justifies the analysis of their magnetic properties in Sec. III. Finally, the calculated ΔH_f^0 are relatively low, similar to those of the recently synthesized PtN_2 crystals.⁶⁰

The calculated equilibrium lattice parameters are given in Table II. For all crystals, the NiAs phase is strongly distorted, i.e., the c/a ratio is considerably larger than the ideal value 1.63. This distortion plays an important role in determining the magnetic properties: for the ideal value of c/a , most of the systems are found to be FM, while the inclusion of the tetragonal distortion destroys the FM order, and the crystals are paramagnetic. In the case of the Zn_3P_2 structure, the c/a ratio is very close to ideal value 1.41, but the internal atomic displacements inside the unit cell are large.

Since $II-V$ compounds in the rs phase are metallic (see Sec. III B) and have the high cubic symmetry, one may expect that the cooperative Jahn-Teller effect takes place and lowers the crystal energy. To check the stability with respect to the Jahn-Teller effect, three types of distortions of the rs structure were considered, namely, (i) a typical tetragonal distortion in the $[001]$ direction (which takes place, e.g., in MnN),^{53,54} (ii) a pseudocubic distortion in the (110) orientation after which the lattice parameters are $a=b=c=a_{eq}$ (rs phase) and $\alpha \neq \beta$, $\gamma=90^\circ$, and (iii) a distortion of the nitrogen sublattice only, in which the N-N distances are reduced from the ideal value $a_{eq}(rs\ phase)/\sqrt{2}$ (which is 3.8 Å in SrN) to 1.1 Å, which is the equilibrium bond length of the N_2 molecule. We have taken into account this distortion because in several nitrides, such as SrN_2 (Ref. 28) or HfN_2 ,⁶¹ N atoms form nearest-neighbor pairs. The obtained results show that the ideal rs phase is stable with respect to all these symmetry-lowering distortions.

Finally, we comment on the possibility of growing FM $II-N$ nitrides. In most cases, the Zn_3P_2 phase is more stable than the rs. However, the different stoichiometries of the two phases imply that the formation of one of them, and, in particular, of the FM rocksalt phase, should strongly depend on the conditions of growth, such as relative flux intensities. Moreover, in epitaxial growth, the substrate and its structure play an important role and determine the structure of the epilayer. Consequently, the choice of appropriate epitaxial conditions should allow obtaining rs- II^A-V nitrides. More specifically, the lattice constants of rs CaN, SrN, and BaN (5.0, 5.4, and 5.55 Å) are close to those of zb-InN (4.98 Å),⁶² zb-GaP (5.45 Å), and zb-GaAs (5.65 Å), respectively, which suggests their use as appropriate substrates.

Also the a_{eq} of rs-CaP (6.24 Å) about only 4% smaller than that of zb-InSb (6.47 Å). The possibility of synthesis of rs- II^A-V nitrides is supported by the growth of metastable phases by molecular-beam epitaxy. This is the case of cubic MnTe or GaN, zb-CrAs,⁴⁶ and zb-CrSb,⁴⁷ to quote a few examples.

V. SUMMARY AND CONCLUSIONS

Using *ab initio* calculations, we have studied magnetic and electronic structures of a number of II^A-V compounds. Four crystal structures were considered: zinc-blende, NiAs, rocksalt, and Zn_3P_2 . In the zb structure, all the considered crystals are characterized by the total spin polarization of free holes. However, the energy of this structure is about 0.3 eV/atom higher than that of the rs phase, in which only CaN, SrN, and BaN nitrides are spin polarized.

To understand the properties of the investigated crystals, we have considered a very broad range of lattice constants, beginning from the case of separated atoms and ending with that of highly compressed solids. A detailed analysis of the electronic structure and density of states revealed that the calculated spin polarization owns its origin to the spin polarization of group-V anions. The atomic spin polarization is the strongest for nitrogen, which may explain the calculated stability of magnetization in CaN, SrN, and BaN nitrides, and the lack of magnetization in rs phosphides, arsenides, and antimonies. Moreover, these results suggest that the observed high-spin states of Si vacancy in SiC,⁷ Ga vacancy in GaP,⁹ as well as the predicted spin polarization of MgO, CaO, and SrO containing a few percent of C (Ref. 11) have the same physical origin, i.e., the pronounced spin polarization of strongly localized s and p orbitals of light atoms. The magnetism of solids observed thus far is related to the presence of transition-metal or rare-earth atoms with partially occupied d or f shells. In the case of II^A-V crystals, the magnetism is related to the partially occupied p shell, and therefore is an alternative mechanism of spin polarization.

Structural stability of II^A-V compounds was analyzed by calculating both their cohesive energies and heats of formation. Cohesive energies of II^A-V nitrides are very close in the rs and Zn_3P_2 phases, and their high values indicate hardness and stability of crystals with respect to decomposition. The calculated heats of formation are lower for the Zn_3P_2 than for the rs structure, which indicates a metastable character of the latter phase. However, the different stoichiometries and lattice parameters of the two phases imply that the potential formation of the FM rocksalt phase should strongly depend on the conditions of epitaxial growth, such as relative flux intensities and the choice of substrates. Appropriate conditions that favor the growth and stabilization of epitaxial layers of FM rs- II^A-V nitrides were specified.

ACKNOWLEDGMENTS

The authors thank Paweł Jakubas for his valuable help in numerical calculations. The calculations were performed at the Interdisciplinary Center for Mathematical and Computational Modeling, Warsaw University.

- ¹D. P. Young, D. Hall, M. E. Torelli, Z. Fisk, J. D. Thompson, H. R. Ott, S. B. Oseroff, R. G. Goodrich, and R. Zysler, *Nature (London)* **397**, 412 (1999).
- ²L. S. Domeles, M. Venkatesan, M. Moliner, L. G. Lunney, and J. M. D. Coey, *Appl. Phys. Lett.* **85**, 6377 (2004).
- ³D. Ceperley, *Nature (London)* **397**, 386 (1999).
- ⁴M. Venkatesan, C. B. Fitzgerald, and J. M. D. Coey, *Nature (London)* **430**, 630 (2004).
- ⁵K. Matsubayashi, M. Maki, T. Tsuzuki, T. Nishioka, and N. K. Sato, *Nature (London)* **420**, 144 (2002).
- ⁶T. Moriwaka, T. Nishioka, and N. K. Sato, *J. Phys. Soc. Jpn.* **70**, 341 (2000).
- ⁷H. Itoh, A. Kawasuso, T. Ohshima, M. Yoshikawa, I. Nashiyama, S. Tanigawa, S. Misawa, H. Okumura, and S. Yoshida, *Phys. Status Solidi A* **162**, 173 (1997).
- ⁸L. Torpo, R. M. Nieminen, K. E. Laasonen, and S. Poykko, *Appl. Phys. Lett.* **74**, 221 (1999).
- ⁹T. A. Kennedy, N. D. Wilsey, J. J. Krebs, and G. H. Stauss, *Phys. Rev. Lett.* **50**, 1281 (1983).
- ¹⁰I. S. Elfimov, S. Yunoki, and G. A. Sawatzky, *Phys. Rev. Lett.* **89**, 216403 (2002).
- ¹¹K. Kenmochi, V. A. Dinh, K. Sato, A. Yanase, and H. Katayama-Yoshida, *J. Phys. Soc. Jpn.* **73**, 2952 (2004).
- ¹²T. L. Makarova, B. Sundquist, R. Hohne, P. Esquinazi, Y. Kopelevich, P. Scharff, V. A. Davidov, L. S. Kashevarova, and A. V. Rakhmanina, *Nature (London)* **413**, 716 (2001).
- ¹³R. A. Wood, M. H. Lewis, M. R. Lees, S. M. Bennington, M. G. Cain, and N. Kitamura, *J. Phys.: Condens. Matter* **14**, L385 (2002).
- ¹⁴B. Narymbetov, A. Omerzu, V. V. Kabanov, M. Tokumoto, H. Kobayashi, and D. Michailovic, *Nature (London)* **407**, 883 (2000).
- ¹⁵P. Esquinazi, A. Setzer, R. Hohne, C. Semmelhack, Y. Kopelevich, D. Spemann, T. Butz, B. Kohlstrunk, and M. Losche, *Phys. Rev. B* **66**, 024429 (2002).
- ¹⁶P. Esquinazi, D. Spemann, R. Hohne, A. Setzer, K.-H. Han, and T. Butz, *Phys. Rev. Lett.* **91**, 227201 (2003).
- ¹⁷Y. Kopelevich, R. R. da Silva, J. H. S. Torres, A. Penicaud, and T. Kyotani, *Phys. Rev. B* **68**, 092408 (2003).
- ¹⁸A. N. Andriotis, M. Menon, R. M. Sheetz, and L. Chernozatonskii, *Phys. Rev. Lett.* **90**, 026801 (2003).
- ¹⁹K. Kusakabe and M. Maruyama, *Phys. Rev. B* **67**, 092406 (2003).
- ²⁰P. O. Lehtinen, A. S. Foster, Y. Ma, A. V. Krasheninnikov, and R. M. Nieminen, *Phys. Rev. Lett.* **93**, 187202 (2004).
- ²¹Y. Ma, P. O. Lehtinen, A. S. Foster, and R. M. Nieminen, *Phys. Rev. B* **72**, 085451 (2005).
- ²²For a review, see S. J. Blundell and F. L. Pratt, *J. Phys.: Condens. Matter* **16**, R771 (2004).
- ²³K. Kusakabe, M. Geshi, H. Tsukamoto, and N. Suzuki, *J. Phys.: Condens. Matter* **16**, 5639 (2004).
- ²⁴M. Sieberer, J. Redinger, S. Khmelevskiy, and P. Mohn, *Phys. Rev. B* **73**, 024404 (2006).
- ²⁵O. Volnianska, P. Jakubas, and P. Bogusławski, *J. Alloys Compd.* **423**, 191 (2006).
- ²⁶K. Sieranski, J. Szatkowski, and J. Misiewicz, *Phys. Rev. B* **50**, 7331 (1994).
- ²⁷J. Gaude, P. L'Haridon, Y. Laurent, and J. Lang, *Rev. Chim. Miner.* **8**, 287 (1971).
- ²⁸G. Auffermann, Yu. Prots, and R. Kniep, *Angew. Chem., Int. Ed.* **40**, 547 (2001).
- ²⁹For a review, see T. Dietl, *Proceedings of the 27th International Conference on Physics Semiconductors*, edited by J. Menendez and C. G. Van de Walle (AIP, New York, 2005), p. 56.
- ³⁰K. W. Edmonds, P. Boguslawski, K. Y. Wang, R. P. Campion, S. N. Novikov, N. R. S. Farley, B. L. Gallagher, C. T. Foxon, M. Sawicki, T. Dietl, M. B. Nardelli, and J. Bernholc, *Phys. Rev. Lett.* **92**, 037201 (2004).
- ³¹H. Saito, V. Zayets, S. Yamagata, and K. Ando, *Phys. Rev. Lett.* **90**, 207202 (2003).
- ³²M. Hickey, C. D. Damsgaard, I. Farrer, S. N. Holmes, A. Husmann, J. B. Hansen, C. S. Jacobsen, D. A. Ritchie, R. F. Lee, G. A. C. Jones, and M. Pepper, *Appl. Phys. Lett.* **86**, 252106 (2005).
- ³³W. H. Wang, M. Przybylski, W. Kuch, L. I. Chelaru, J. Wang, Y. F. Lu, J. Barthel, H. L. Meyerheim, and J. Kirschner, *Phys. Rev. B* **71**, 144416 (2005).
- ³⁴J. P. Perdew, K. Burke, and M. Ernzerhof, *Phys. Rev. Lett.* **77**, 3865 (1996).
- ³⁵<http://www.pwscf.org>
- ³⁶D. Vanderbilt, *Phys. Rev. B* **41**, 7892(R) (1990).
- ³⁷P. Boguslawski and J. Bernholc, *Phys. Rev. B* **72**, 115208 (2005).
- ³⁸We do not consider other AFM phases since, e.g., in zb-MnTe energies of type-I and type-III AFM orders differ by 2 meV/atom only, see P. Djemia, Y. Roussigné, A. Stashkevich, W. Szuszkiewicz, N. Gonzalez Szwacki, E. Dynowska, E. Janik, B. J. Kowalski, G. Karczewski, P. Boguslawski, M. Jouanne, and J. F. Morhange, *Acta Phys. Pol. A* **106**, 239 (2004). Similar results are expected for II-V compounds. This value is an order of magnitude smaller than $\Delta E^{\text{FM-AFM}}$ for CaN and SrN, and thus does not affect our conclusions.
- ³⁹We notice that the energy of spin polarization of isolated anions is an order of magnitude larger than that in crystals, which follows, in particular, from screening and hybridization effects, and a different occupation of the p (anion) shell in the two cases.
- ⁴⁰A. Harrison, *Electronic Structure and the Properties of Solids* (W. H. Freeman and Company, San Francisco, 1980).
- ⁴¹V. A. Gubanov, A. I. Liechtenstein, and A. V. Postnikov, *Magnetism and the Electronic Structure of Crystals* (Springer, Berlin, 1992).
- ⁴²D. M. Ceperley and B. J. Alder, *Phys. Rev. Lett.* **45**, 566 (1980).
- ⁴³G. Ortiz, M. Harris, and P. Ballone, *Phys. Rev. Lett.* **82**, 5317 (1999).
- ⁴⁴B.-G. Liu, *Phys. Rev. B* **67**, 172411 (2003).
- ⁴⁵A. K. Das, C. Pampuch, A. Ney, T. Hesjedal, L. Daweritz, R. Koch, and K. H. Ploog, *Phys. Rev. Lett.* **91**, 087203 (2003).
- ⁴⁶M. Mizuguchi, H. Akinaga, T. Manago, K. Ono, M. Oshima, M. Shirai, M. Yuri, H. J. Lin, H. H. Hsieh, and C. T. Chen, *J. Appl. Phys.* **91**, 7917 (2002).
- ⁴⁷J. H. Zhao, F. Matsukura, K. Takamura, E. Abe, D. Chiba, and H. Ohno, *Appl. Phys. Lett.* **79**, 2776 (2001).
- ⁴⁸J. E. Pask, L. H. Yang, C. Y. Fong, W. E. Pickett, and S. Dag, *Phys. Rev. B* **67**, 224420 (2003).
- ⁴⁹H. F. George and H. K. John, *Phys. Rev.* **93**, 1004 (1954).
- ⁵⁰D. Gall, I. Petrov, N. Hellgren, L. Hultman, J. E. Sundgren, and J. E. Greene, *J. Appl. Phys.* **84**, 6034 (1998).
- ⁵¹T.-Y. Lee, D. Gall, C.-S. Shin, N. Hellgren, I. Petrov, and J. E. Greene, *J. Appl. Phys.* **94**, 921 (2003).
- ⁵²J. R. Frederick and D. Gall, *J. Appl. Phys.* **98**, 054906 (2005).
- ⁵³K. Suzuki, T. Kaneko, H. Yoshida, Y. Obi, H. Fujimori, and H.

- Morita, J. *Alloys Compd.* **306**, 66 (2000).
- ⁵⁴H. Yang, H. Al-Britthen, A. R. Smith, J. A. Borchers, R. L. Capelletti, and M. D. Vaudin, *Appl. Phys. Lett.* **78**, 3860 (2001).
- ⁵⁵W. R. L. Lambrecht, M. Prikhodko, and M. S. Miao, *Phys. Rev. B* **68**, 174411 (2003).
- ⁵⁶B. R. Sahu and L. Kleinman, *Phys. Rev. B* **68**, 113101 (2003).
- ⁵⁷A. Janotti, S. H. Wei, and L. Bellaïche, *Appl. Phys. Lett.* **82**, 766 (2003).
- ⁵⁸P. Bogusławski and J. Bernholc, *Appl. Phys. Lett.* **88**, 092502 (2006).
- ⁵⁹N. Takeuchi, *Phys. Rev. B* **65**, 045204 (2002).
- ⁶⁰J. C. Crowhurst, A. F. Goncharov, B. Sadigh, Ch. L. Evans, P. G. Morrall, J. L. Ferreira, and A. J. Nelson, *Science* **311**, 1275 (2006).
- ⁶¹R. Yu and X. F. Zhang, *Phys. Rev. B* **72**, 054103 (2005).
- ⁶²A. Tabata, A. P. Lima, L. K. Teles, L. M. R. Scolfaro, J. R. Leite, V. Lemos, B. Schottker, T. Frey, D. Schikora, and K. Lischka, *Appl. Phys. Lett.* **74**, 362 (1999).